Proceedings of the 12th International Conference "Ion Implantation and Other Applications of Ions and Electrons", ION 2018

Structure and Hardness Evolution of Silicon Carbide Epitaxial Layers Irradiated with He^+ Ions

V.V. Pilko[a,*], F.F. Komarov[a] and P. Budzynski[b]

[a]Institute of Applied Physics Problems, 7 Kurchatov Street, 220045 Minsk, Belarus

[b]Lublin University of Technology, 36 Nadbystrzycka Street, 20-618 Lublin, Poland

In our study, the 4H polytype SiC epitaxial layers of ~ 3 μm thickness on SiC substrates were implanted with 500 keV He^+ ions fluences in the range from 5×10^{14} ion/cm^2 to 1×10^{17} ion/cm^2. The induced defect distributions were studied by means of the Rutherford Backscattering technique in the channeling regime (RBS/C). Structure changes were identified via characteristic phonons intensity deviations registered by the Raman Spectroscopy technique. Evolution of hardness for all irradiated samples was investigated by means of conventional Vickers measurements and dynamic nanoindentation with the Oliver–Pharr method of results processing. For all samples, the normal indentation size effect was observed.

DOI: 10.12693/APhysPolA.136.351

PACS/topics: 61.80.Jh, 62.20.Qp

1. Introduction

Silicon carbide is a material of vital importance in several applications such as nuclear fission and fusion reactor projects, reliable radiation–resistant diagnostic sensors and radiation detectors. All these applications assume harsh influence of radiation that drastically changes intrinsic physical properties of materials. Particularly fission and transmutation reaction products such as He induces volumetric and tribomechanical properties deterioration that can lead to crucial consequences in such an environmental sensitive field as nuclear energetics.

2. Experiment details

In this paper, single-crystal standard epitaxial layers with {0001} direction of 8° off–axis orientation towards the ⟨1120⟩ of 4H–SiC on SiC substrates obtained from CREE (Durham, USA) were used. The epilayers thickness was ~ 3 μm. Quality of the epitaxial layers was estimated by minimizing backscattered 1.5 MeV He ions yield in the channeling regime up to 30 times in comparison with the random one. Epitaxial layers were implanted with 500 keV He^+ ions at room temperature with incident ion beam normal to the substrate plane. To improve implantation uniformity all irradiations were performed in a broad beam mode applying the triangle shaped modulating voltage to the sets of deflection plates with frequencies of 15 and 4 Hz in the horizontal and vertical directions, respectively. The overall beam extension due to this perturbation did not exceed 15% compared to the initial beam. The implantation fluences were: 5×10^{14}, 1×10^{15}, 5×10^{15}, 1×10^{16}, 5×10^{15}, and 1×10^{17} ion/cm^2 to cover all distinctive ranges of radiation induced defects concentration. Ion channeling spectra (Fig. 1) were collected ex-situ by the Van de Graaff accelerator with 1.5 MeV $^4He^+$ ions incident along the {0001} direction and backscattered into a detector at 170° with respect to the incident beam direction. Raman spectra were measured using a Bruker Senterra Raman spectrometer coupled with an Olympus microscope that contains an x–y–z stage. The 532 nm line of a frequency-doubled Nd:YAG laser was focused on a 1 μm spot and collected through a 50x objective. Spectra were recorded in the range 700–1100 cm^{-1} with a spectral resolution of about 5–7 cm^{-1}. Nanoindentation tests were performed using CSM Ultra Nano Hardness Tester (UNHT) with the Berkovich diamond indenter coupled with a microscope with digital camera. The values of hardness and elastic modulus of the samples were calculated using the UNHT software.

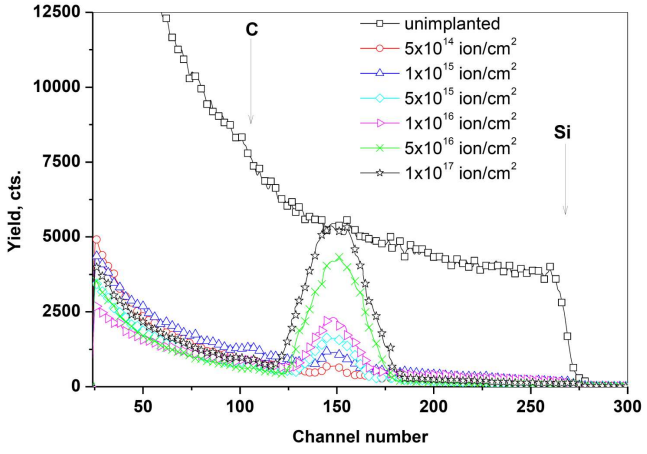

Fig. 1. Aligned RBS spectra in channeling direction for 4H–SiC bombarded with 500 keV He^+ ions in a fluence range from 5×10^{14} ion/cm^2 to 1×10^{17} ion/cm^2 and random RBS spectrum for unimplanted 4H–SiC.

*corresponding author; e-mail: pilkowladimir@gmail.com

The hardness (H) was calculated using the relation

$$H = \frac{F}{A}, \tag{1}$$

where F is the applied force, A is the projected indentation impression area determined from the contact depth using the Oliver-Pharr method [1].

Elastic modulus (E) was calculated from the relation

$$\frac{1}{E_{\text{eff}}} = \frac{1-\nu_s^2}{E} + \frac{1-\nu_i^2}{E_i}, \tag{2}$$

where ν_s and ν_i are the Poisson ratios of the sample and indenter, respectively, E_i is the elastic modulus of the indenter. The Poisson ratio of the sample $\nu_s = 0.19$ [2]. E_{eff} is the Young modulus calculated from the tangent $\mathrm{d}F/\mathrm{d}h$ fit of unloading part of the load — displacement curve [3]:

$$E_{\text{eff}} = \frac{\sqrt{\pi}}{2\beta\sqrt{A}} \frac{\mathrm{d}F}{\mathrm{d}h}, \tag{3}$$

where β is the geometrical factor of the indenter.

Micro indentation tests were performed using the Vickers hardness tester (Durascan 20), and in doing so, the indentation diagonals for the hardness evaluation were measured. Each indentation was made at a load of 0.1 N with a dwell time of 15 s.

3. Results and discussion

Figure 1 presents the RBS-C spectra of 4H–SiC irradiated with different fluences at room temperature. Rise of relative structure disorder with the increasing ion dose is observed for all implanted samples. Relatively low surface peaks are observed in contrast to the cases of other non-metals such as Si, GaN, and ZnO [4], which show a very limited role of surface in the damage accumulation for these irradiation conditions and ion type. Indeed, the surface peaks for SiC are almost indistinguishable compared to the bulk peaks and there are no significant anomalies in the near-surface region. As follows from Fig. 1, all the measured damage build up curves are very close to the normal distribution. For all implanted samples, the bulk defect peaks are located at around 1.3 μm which is close to the depth where the profile of generated vacancies has its maximum according to the SRIM simulations and shape of damage profile is close to that obtained via RBS measurements.

The penetration length at which 532 nm laser intensity decreases by $\sim$ 2.72 times in 4H–SiC is about 20 μm. Therefore this magnitude covers the damage regions fully (peak at 1.23 μm according to SRIM calculations). The corresponding peak dpa (displacement per atom) numbers of irradiated samples from low to high are: 0.021, 0.042, 0.21, 0.42, 2.10, and 4.20. Figure 2 shows the Raman spectra of 4H–SiC samples before and after irradiation. The spectrum of not irradiated sample shows two featured peaks. They are consistent with the first-order Raman scattering of 4H–SiC [5], including a strong transverse optical (TO) peak at 777 cm^{-1}, and a weak longitudinal optical (LO) peak at 984 cm^{-1}. For the sample irradiated to 0.021 dpa (5×10^{14} ion/cm^2), the spectrum is similar to that of the not irradiated one, suggesting that the sample is only slightly damaged. With increasing dpa the intensity of TO peaks decreases, indicating the decomposition of some crystalline ordered Si-C bonds. For the samples irradiated at the highest dpa numbers (2.10 and 4.20), the Raman spectrum shows noticeable differences. Several crystalline peaks of SiC are not visible anymore and according to [6] two new broad peaks related to different C structures are supposed to appear corresponding to the sp^2 bonding in nanocrystalline graphite and C^3_{sp}–C^3_{sp}/sp^2 bonds.

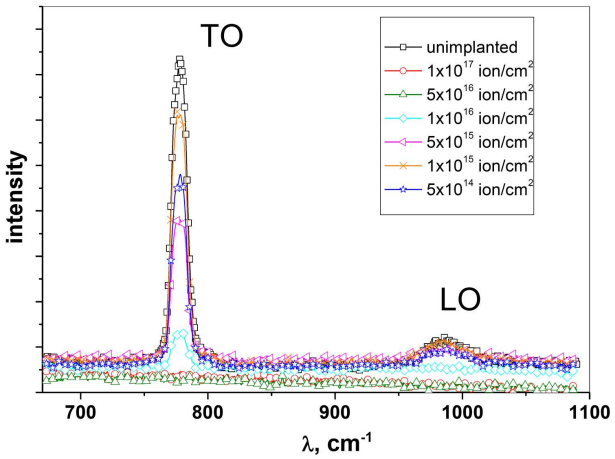

Fig. 2. Raman spectra of 4H–SiC samples irradiated with fluence values 5×10^{14}, 1×10^{15}, 5×10^{15}, 1×10^{16}, 5×10^{15}, and 1×10^{17} ion/cm^2.

Figure 3 shows the load-displacement curves for sample 1 (1×10^{17} ion/cm^2) and 2 (5×10^{16} ion/cm^2) for five maximum test loads (5 mN, 10 mN, 15 mN, 20 mN, 30 mN). For the sample 1, high amounts of elastic recovery can be seen in the unloading curve indicating only elastic deformation. Therefore, analysis of the unloading curve enables to define an elastic modulus of the tested samples. A similar effect was observed for all samples except sample 2. For sample 2 there is a little elastic displacement in the unloading curve indicating mainly plastic deformation.

For the indentation, the hardness variations can be explained by the indentation size effect (ISE) [3]. For all samples, the normal ISE was observed [7] (hardness decreases with the increasing penetration depth).

Analysis of the experimental data on hardness as a function of indentation depth is performed according to the following relation

$$H^2 = H_0^2 \left(1 + \frac{h^*}{h}\right), \tag{4}$$

where h^* is the length characterizing the depth dependence of the hardness. Transforming Eq. (4), the following relation can be written

$$H^2 = H_0^2 h^* \left(\frac{1}{h_m}\right) + H_0^2. \quad (5)$$

From the dependence of H^2 versus the reverse of the maximum penetration depth h_m, a good straight line is found, and the independent hardness of the sample H_0 depending on the applied load was determined. The values of H_0 for all samples are listed in Table I.

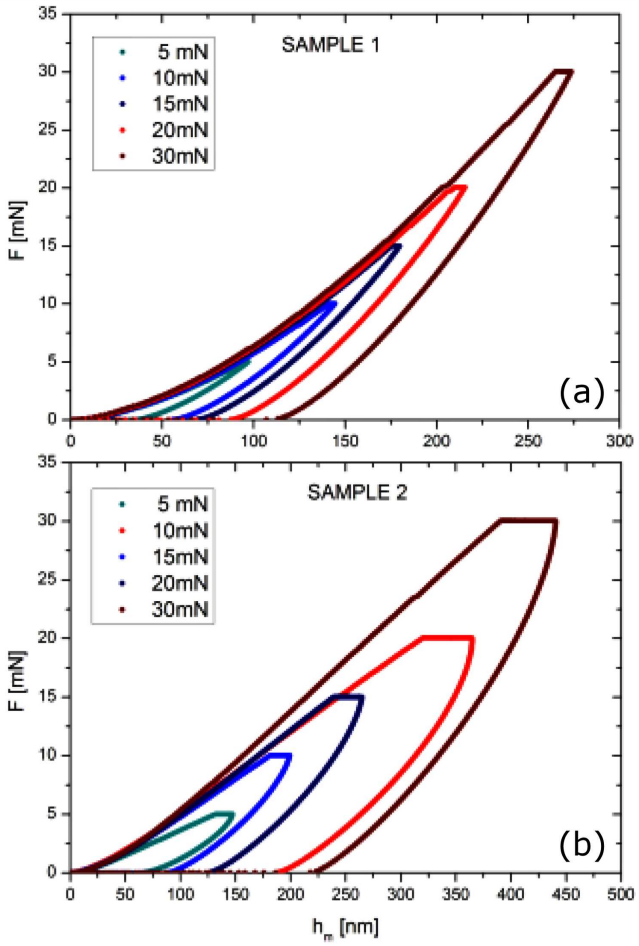

Fig. 3. Examples of typical load-displacement F–h curves of implanted SiC for samples 1 and 2.

TABLE I

Values of independent hardness H_0 for all samples

Sample	Independent hardness (H_0) [GPa]
1 (1×10^{17} ion/cm^2)	35.8
2 (5×10^{16} ion/cm^2)	9.36
3 (1×10^{16} ion/cm^2)	20.67
4 (5×10^{15} ion/cm^2)	30.64
5 (1×10^{15} ion/cm^2)	18.41
6 (5×10^{14} ion/cm^2)	24.7

The experimental results of nanohardness H versus the maximum penetration depth h_m for five maximum test loads (5 mN, 10 mN, 15 mN, 20 mN, 30 mN) performed on the implanted SiC layers at the loading/unloading rates: 5mN/min, 10 mN/min, 15 mN/min, 20 mN/min, and 30 mN/min at a dwell time of 10 s and maximum load, respectively are presented in Fig. 4.

The hardness value decreases with the increasing penetration depth. That means that in all samples the normal ISE was observed. For sample 1 implanted with the ion fluence 1×10^{17} ions/cm^2, the average hardness values are between 37.8 GPa for the maximum test load 5 mN and 36.3 GPa for the maximum test load 30 mN. For sample 2 implanted with the ion fluence 5×10^{16} ions/cm^2, the average hardness values are between 14.75 GPa for the maximum test load 5 mN and 11.22 GPa for the maximum test load 30 mN. The average hardness of the sample 3 implanted with the ion fluence 1×10^{16} ions/cm^2 is 25.78 GPa at the lowest depth and decreases to 21.55 GPa at the maximum depth. For sample 4 implanted with the ion fluence 5×10^{15} ions/cm^2, the average hardness values are between 35.55 GPa for the maximum test load 5 mN and 31.59 GPa for the maximum test load 30 mN. For sample 5 implanted with the ion fluence 1×10^{15} ions/cm^2, the average hardness values are between 70.73 GPa for the maximum test load 5 mN and 38.58 GPa for the maximum test load 30 mN. In all samples, the linear dependence of nanohardness H on the maximum penetration depth h_m was observed, with the exception of the obtained results from sample 5 (1×10^{15} ion/cm^2) for which the exponential dependence was obtained.

Figure 5 shows the dependence of the conventional Vickers hardness on the irradiation fluence. The hardness slightly decreases with the increment of irradiation fluence. These results are in good agreement with those obtained in [8] or [9]. As soon as conventional Vikkers hardness measurements are less sensitive to nanoscale effects and give us the general view about hardness evolution of the whole sample (irradiated epitaxial layers plus SiC substrate), the hardness values obtained by this method are much more comparable to those representative for bulk SiC. Still, the irradiation effects can be clearly seen.

The value of Young modulus (results not presented in the graphic form) also decreases with the increasing penetration depth. For sample 1, the average Young modulus values are between 371.0 GPa for the maximum test load 5 mN and 318.9 GPa for the maximum test load 30 mN. For sample 2, the average Young modulus values are between 220.77 GPa for the maximum test load 5mN and 161.99 GPa for the maximum test load 30 mN. The average Young modulus of the sample 3 is 322.79 GPa at the lowest depth and decreases to 216.3 GPa at the maximum depth. For sample 4 the average Young modulus values are between 374.3 GPa

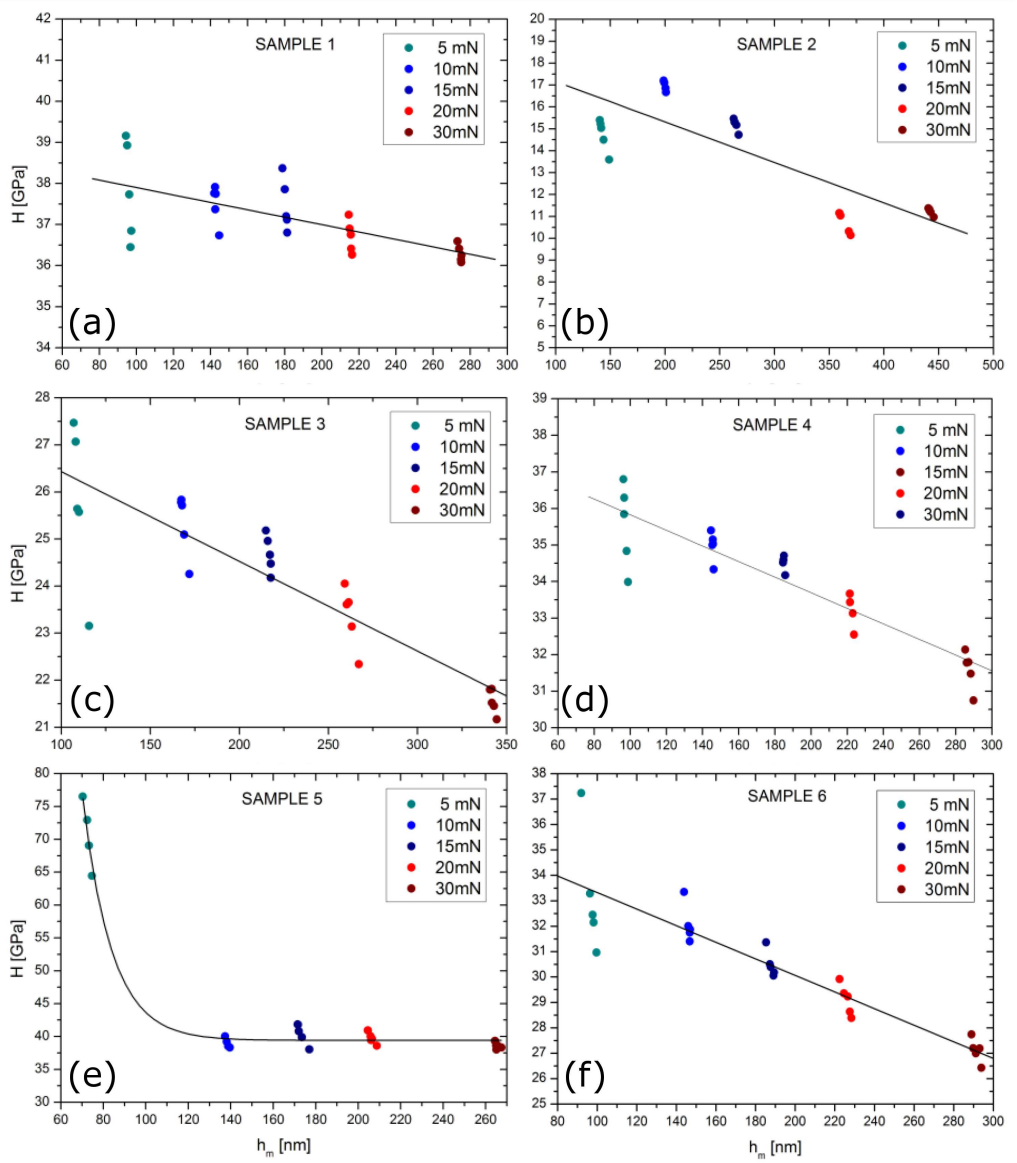

Fig. 4. Dependence of indentation hardness H on maximum penetration depth h_m for five different loads.

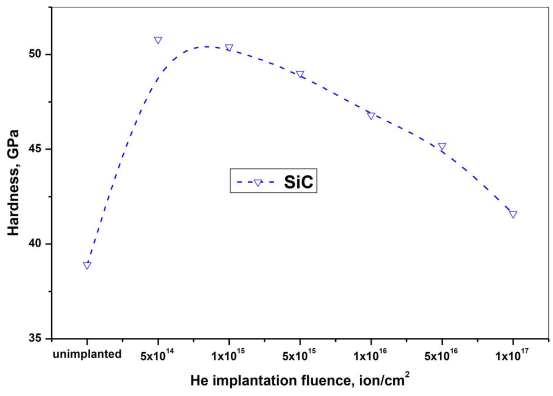

Fig. 5. Dependence of microhardenss on implantation fluence for SiC samples.

for the maximum test load 5mN and 303.23 GPa for the maximum test load 30 mN. For sample 5 the average Young modulus values are between 697.7 GPa for the maximum test load 5mN and 354.0 GPa for the maximum test load 30 mN. For sample 6 the average Young modulus values are between 415.8 GPa for the maximum test load 5 mN and 353.8 GPa for the maximum test load 30 mN.

4. Conclusions

The hardness and elastic modulus of the epitaxial 4H–SiC after 500 keV He^+ ions irradiation up to 0.021, 0.042, 0.21, 0.42, 2.10, and 4.20 dpa (the corresponding fluences are: 5×10^{14}, 1×10^{15}, 5×10^{15}, 1×10^{16}, 5×10^{15}, and 1×10^{17} ion/cm^2) at room temperature were evaluated using two indentation techniques. Using

the conventional Vickers hardness measurements small hardness decrease with the increment of irradiation fluence was observed. As for the nanoindentation tests, subtle effects of hardness dynamics that can represent evolution of defects formation and He atom accumulation were observed. They are a matter of concern regarding our future studies of the epitaxial SiC structure evolution upon irradiation with He ions.

References

[1] W.C. Oliver, G.M. Pharr, *J. Mater. Res.* **7**, 1564 (1992).

[2] J.F. Shackelford, Y.H. Han, S. Kim, S.H. Kwon, in: *CRC Materials Science and Engineering Handbook*, Eds. CRC Press, 2015.

[3] W.D. Nix, H. Gao, *J. Optoelectron. Adv. Mater.* **12**, 2082 (2010).

[4] S.O. Kucheyev, J.S. Williams, C. Jagadish, J. Zou, G. Li, *Phys. Rev. B* **62**, 7510 (2000).

[5] K. Karch, P. Pavone, W. Windl, O. Schutt, D. Strauch, *Phys. Rev. B* **50**, 17054 (1994).

[6] L. Min, Y. Xinmei, G. Yantao, L. Renduo, H. Hefei, Z. Xingtai, T.K. Sham, *J. Eur. Ceramic Soc.* **37**, 1253 (2017).

[7] W.D. Nix, H. Gao, *J. Mech. Phys. Solids* **46**, 411 (1998).

[8] T. Yang, H. Zang, C. He, D. Guo, P. Zhang, J. Xi, Li Ma, *Int. J. Appl. Ceram. Technol.* **12**, 390 (2015).

[9] S. Nogami, A. Hasegawa, *IOP Conf. Series: Mater. Sci. Eng.* **18**, 162007 (2011).